Dynamics of freshwater-seawater mixing zone development in dual-domain formations

Chunhui Lu[1] and Jian Luo[1]

Received 25 March 2010; revised 1 September 2010; accepted 24 September 2010; published 23 November 2010.

[1] Dynamic responses of freshwater-seawater mixing zones to seasonal freshwater-level fluctuations and the presence of kinetic mass transfer between mobile and immobile domains have been analyzed using numerical models. Mixing enhancement is mainly controlled by the unsynchronized behavior of concentration distributions in the mobile and immobile domain. Such effect is maximized at the aquifer bottom when the retention timescale (the reciprocal of mass transfer rate) in the immobile domain is comparable to the period of freshwater-level fluctuations. Kinetic mass transfer may alter the time lag between periodic freshwater-level fluctuations and the movement of the mixing zone, causing the expansion and contraction of the mixing zone. Mixing enhancement by kinetic mass transfer is nonuniform in the mixing zone, and the mixing zone thickness may vary significantly within a period. By contrast, large dispersion coefficients may create thicker mixing zones but may not cause such unsynchronized behavior and alter the time lags of different concentration contour lines; that is, the mixing enhancement is rather uniform in the mixing zone. The dynamics of mixing zone development is sensitive to the flow velocity, which is influenced by the hydraulic conductivity, amplitude of the freshwater-level fluctuations, and the capacity ratio of kinetic mass transfer.

Citation: Lu, C., and J. Luo (2010), Dynamics of freshwater-seawater mixing zone development in dual-domain formations, *Water Resour. Res.*, *46*, W11601, doi:10.1029/2010WR009344.

1. Introduction

[2] The mixing zone developed at freshwater-seawater interfaces is one of the most important features in complex coastal hydrogeologic systems [e.g., *Cooper et al.*, 1964, *Robinson et al.*, 2007a]. Across the mixing zone, the salt concentration and fluid density vary between those of freshwater and seawater. The density gradient within the mixing zone causes the rise of diluted saltwater, overlaying seawater, and results in flow circulation as the seawater moves toward the mixing zone to replace the diluted saltwater. Understanding the dynamics of mixing zone development under various hydrogeologic conditions is essential for designing effective management strategies of groundwater resources and implementing sustainable stewardship of coastal and offshore environments.

[3] The present research aims to numerically investigate the dynamic process of mixing zone development in a dual-domain subsurface medium. Kinetic mass transfer between relatively mobile fluids and fluids in stagnant pores occurs in almost all fractured and porous media over various scales ranging from pore scale to field scale, and has significant implications on coastal groundwater management. For example, the aquifer storage and recovery (ASR) strategy may have a low recovery ratio in a dual-domain coastal aquifer due to the mobilization of solutes initially residing in immobile domains [*Eastwood and Stanfield*, 2001; *Culkin et al.*, 2008]. Our previous study has found that kinetic mass transfer combined with periodic movement of the mixing zone may significantly enhance mixing and result in a much thicker mixing zone, as shown in Figure 1 [*Lu et al.*, 2009]. Prior to our finding, thick mixing zones were usually characterized by large dispersion coefficients or assuming highly heterogeneous hydraulic conductivity fields, both of which may not be realistic [*Dagan*, 2006]. In this note, we further illustrate the dynamic process of mixing enhancement for a periodically moving mixing zone in the presence of kinetic mass transfer. Specifically, the dynamic behavior of spatial and temporal distributions of the mixing zone, including the concentration distributions in both mobile and immobile domains, the movement of different contour lines, and the time lag between freshwater fluctuations and the mixing zone responses, are investigated in various hydrogeologic conditions and compared with the case assuming large dispersion coefficients. Such findings and results will lead to improved understanding of the mechanisms responsible for thick mixing zones and transport processes associated with the mixing zone development, such as seawater intrusion, submarine groundwater discharge and geochemical reactive processes.

2. Numerical Method

[4] A typical two-dimensional domain (see Figure 1) is set up to represent a cross-shore transect of an unconfined coastal aquifer with a length of 200 m, a thickness of 35 m,

[1]School of Civil and Environmental Engineering, Georgia Institute of Technology, Atlanta, Georgia, USA.

0043-1397/10/2010WR009344

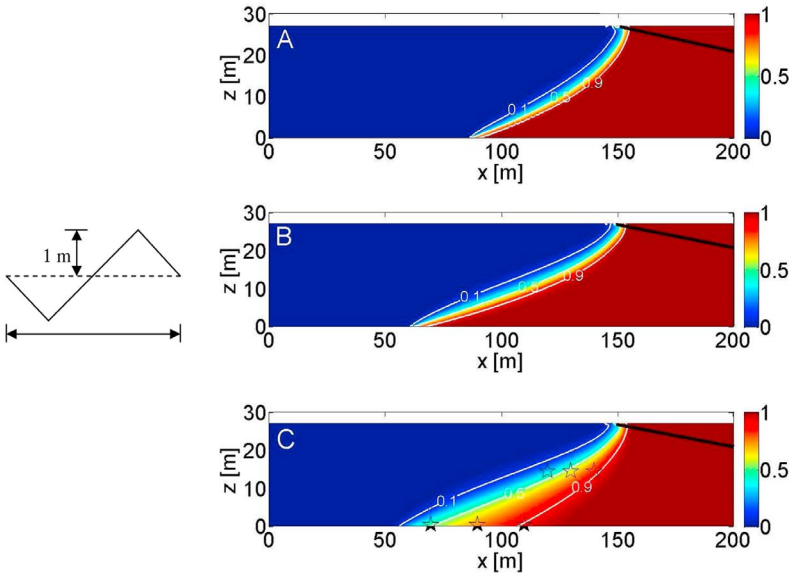

Figure 1. Numerical simulations of freshwater-seawater mixing zone in an unconfined aquifer. (a) Steady state normalized concentration distribution in the absence of kinetic mass transfer; (b) normalized concentration distribution of a transient simulation without kinetic mass transfer; and (c) normalized concentration distribution of a transient simulation with kinetic mass transfer at the time event when the freshwater boundary (left boundary) equals the mean freshwater head. The thick black lines represent the coastal beach with a slope of 0.1. The mixing zones are characterized by three normalized concentration contour lines: 0.1, 0.5 and 0.9. The stars in Figure 1c represent six observation points at the elevations of 0 and 15 m.

and a beach slope of 0.1, similar to previously reported numerical experiments [*Michael et al.*, 2005; *Robinson et al.*, 2006, 2007b; *Lu et al.*, 2009]. A base model is first built by defining the following hydrogeologic conditions. The aquifer is isotropic and homogeneous with a hydraulic conductivity of 30 m d^{-1} and both mobile and immobile porosities being 0.2, which represent a unitary capacity ratio of mass transfer, defined as the ratio between the immobile and mobile porosity. The longitudinal and transverse dispersivity are 0.5 and 0.05 m, respectively. Seasonal freshwater-level fluctuations are imposed at the landward vertical boundary (left boundary in Figure 1) by defining a triangular, periodic hydraulic head variation with the amplitude $A = 1$ m and the period $T = 360$ d. The use of the triangular function instead of a sinusoid function is to minimize the pressure periods required to reproduce the periodic function [*Zhang et al.*, 2001; *Brovelli et al.*, 2007]. The first-order mass transfer rate coefficient is 0.0028 d^{-1}, which implies a retention timescale in the immobile domain, defined as the reciprocal of the first-order mass transfer rate coefficient, equal to the period of freshwater fluctuations. At the seaward vertical boundary (right boundary in Figure 1), constant hydraulic head and salt concentration are assigned because tidal activities have a much shorter period and may hardly cause the movement of the mixing zone in a large-scale simulation [*Cartwright et al.*, 2004; *Michael et al.*, 2005]. The mean hydraulic gradient between the landward vertical boundary and the coastline is 0.0067. The upper boundary in the aquifer is phreatic surface with negligible groundwater recharge, and the bottom is a no-flow boundary.

[5] A miscible fluid model is applied to simulate the mixing zone development in a dual-domain coastal aquifer. Flow and transport is coupled by a linear relationship between density and concentration in the mobile domain. SEAWAT-2000 [*Langevin et al.*, 2003] is used to simulate the variable-density flow and transport described above. The entire domain is divided into two zones: an ocean zone and an aquifer zone, which are separated by the slanted beach. A high hydraulic conductivity (10^3 m d^{-1}), an effective porosity $n_e = 1$, and a constant saltwater concentration of 35 kg m^{-3} are assigned to the ocean zone. A horizontal strip of cells with the same boundary conditions at the seaward vertical boundary are added on the top of the ocean surface to reproduce the flat surface of the ocean [*Brovelli et al.*, 2007; *Robinson et al.*, 2007b]. The entire domain is discretized into a uniform grid with a cell size of 0.5 m × 0.5 m, yielding 28,000 cells in total. This grid spacing corresponds to a local Peclet number of 1.

[6] The following numerical experiments are conducted: (1) steady state simulations for the base model with and without mass transfer; (2) transient simulations for the base model with periodic freshwater-level fluctuations; and (3) transient simulations by varying a series of parameters, including hydraulic conductivity, dispersion coefficients, amplitude of freshwater fluctuations, and mass transfer coefficients. All transient simulations start from steady state simulations, and terminate after the salt concentration distribution reaching a dynamic equilibrium state; that is, the tolerance of the maximum concentration variation is satisfied when doubling the computation period. For simplicity, we use three normalized salt concentration contour lines,

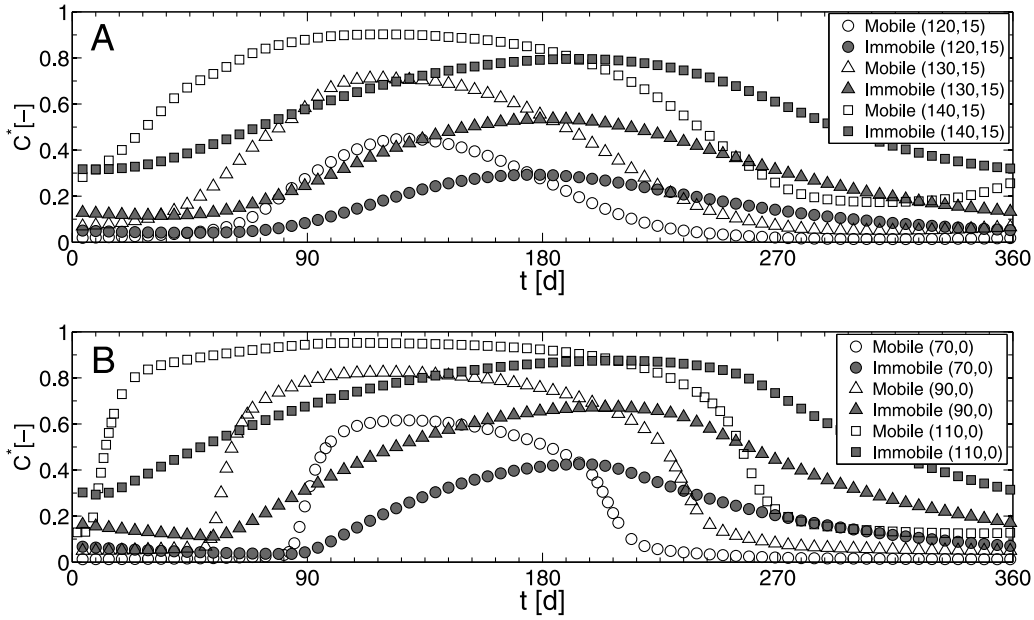

Figure 2. Temporal profiles of concentrations in the mobile and immobile domain at six observation points in the presence of kinetic mass transfer and periodic freshwater fluctuations. The period starts at the moment of falling water level: (a) (120, 15), (130, 15), and (140, 15) and (b) (70, 0), (90, 0), and (110, 0). Coordinate units are meters.

0.1, 0.5 and 0.9, to describe the movement and distribution of the mixing zone.

3. Results and Discussion

[7] Mixing of freshwater and seawater is enhanced primarily due to the unsynchronized behavior of concentrations in the mobile and immobile domain. Two mixing zones may be defined in a dual-domain medium: one in the mobile domain, and the other in the immobile domain. There is an overlap between these two mixing zones, but they do not exactly coincide. The nonequilibrium concentrations in the mobile and immobile domain create the driving force for mass transfer and mixing enhancement.

[8] Figure 2 illustrates this process within one period (see the period in Figure 1) by analyzing the temporal profiles of concentrations at six points at different elevation, (120, 15), (130, 15), (140,15), (70, 0), (90, 0), and (110, 0), in which the first three are approximately located at the medium depth of the water level, and the remaining points are located at the bottom of the aquifer where the mixing enhancement is the most significant (see Figure 1). At the beginning of the period, nonequilibrium concentrations in the mobile and immobile domains drive mass transfer from the immobile domain to the mobile domain, causing slowly increasing mobile concentrations and slowly decreasing immobile concentrations. With the decrease of the freshwater level, significant landward movement of the mixing zone causes a fast increasing concentration in the mobile domain, which results in a fast increasing concentration in the immobile domain due to enhanced mass transfer driving forces. Maximum concentrations in the mobile domain occur in the second quarter. After that, the mobile concentration gradually decreases as a result of mass transfer, while the immobile concentration keeps rising until these two become equal. When the hydraulic gradient is reversed as a result of the rise of the freshwater level, seaward movement of the mixing zone causes significant dilution and a fast decreasing mobile concentration. The immobile concentration then decreases due to the reversed mass transfer process. The point at (110, 0), the closest point to the seaward boundary, has the longest period for salt transferred from the mobile domain to the immobile domain because it is the first to receive intruded saltwater with the landward movement of the mixing zone and the last to be diluted as the mixing zone retreats seaward. Contrarily, points closer to the freshwater boundary have shorter periods of mass transfer from the mobile domain to the immobile domain because they receive saltwater later as seawater intrusion progresses, and are diluted earlier by the freshwater with the seaward movement of the mixing zone. Furthermore, the profiles at different depth show similar temporal patterns, but at the shallower depth the concentrations in the mobile domain change relatively more gently than those at the bottom, indicating variable movement range of the mixing zone and different degree of mixing enhancement at different depth.

[9] Figure 3 illustrates the impacts of hydrogeologic conditions on the dynamics of the mixing zone development by the temporal and spatial distributions of three concentration contour lines, 0.1, 0.5 and 0.9.

[10] Figure 3a shows the base model results: (1) the movement of different contour lines in response to freshwater fluctuations is unsynchronized due to kinetic mass transfer, resulting in significantly varying moving ranges for different contour lines, by a factor of 4, and (2) a time lag exists between freshwater-level fluctuations and the movement of the mixing zone.

[11] Figure 3b shows that the mixing zone in the case with larger dispersivities (Figure 3b, right) is thicker than that with smaller dispersivities (Figure 3b, left) in the absence of kinetic mass transfer. However, the enhanced thickness of the mixing zone is nearly uniform within a period for both

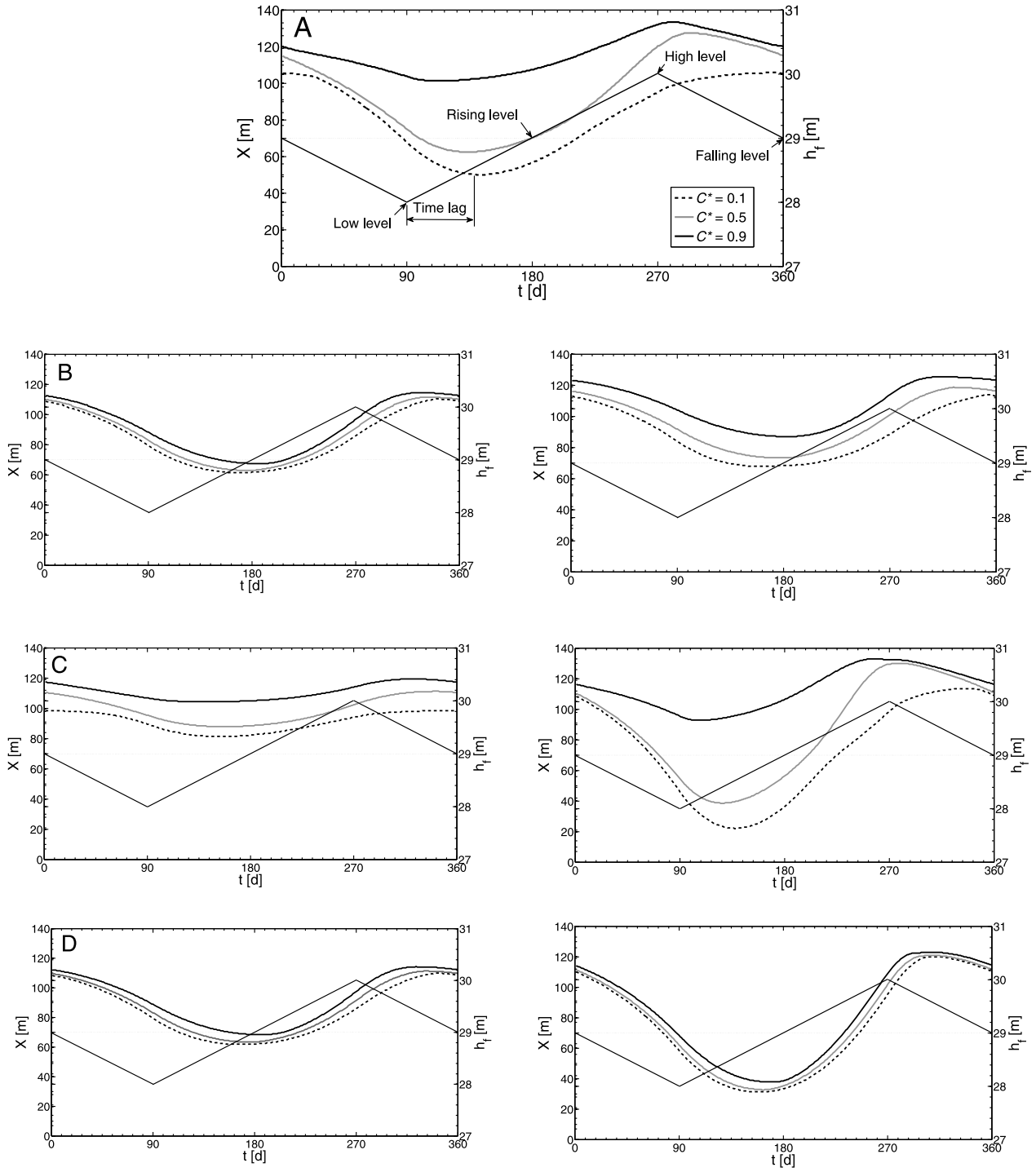

Figure 3. The dynamics of mixing zone development influenced by hydrogeologic conditions, including dispersion, hydraulic conductivity, and mass transfer rate coefficient. Temporal and spatial evolution of the mixing zone distribution is characterized by three normalized concentration contour lines at the aquifer bottom (left y axis) corresponding to periodic freshwater fluctuations (right y axis). (a) The base model with defined parameters: hydraulic conductivity 30 m d^{-1}, first-order mass transfer rate coefficient 0.0028 d^{-1}, which corresponds to a unitary timescale ratio between the retention in the immobile domain and the period of freshwater fluctuations, and longitudinal and transverse dispersivities 0.5 m and 0.05 m, respectively. (b) The impact of dispersion for (left) the base model without kinetic mass transfer and (right) the base model with larger dispersivities (2.5 m and 0.25 m) and without kinetic mass transfer. (c) The impact of hydraulic conductivity for the base model with hydraulic conductivity (left) 10 m d^{-1} and (right) 50 m d^{-1}. (d) The impact of mass transfer rate coefficient for a timescale ratio of (left) 0.01 and (right) 100.

cases without mass transfer. This indicates synchronized behavior for different contour lines in response to freshwater fluctuations, resulting in similar moving ranges for different contour lines. Specifically, the 0.5 contour line remains almost at the middle of the mixing zone for the cases without mass transfer, but approaches the 0.1 contour line when the mixing zone expands and the 0.9 contour line when the mixing zone shrinks for the case with mass transfer. Because the freshwater level drops from the mean level at the beginning of a period, one may expect that the maximum landward movement of the mixing zone occurs at the end of the second quarter when the freshwater level rises to the mean level from the lowest level, which implies a 3 month time lag between the freshwater level variation and the mixing zone movement. With the consideration of mass transfer, this time lag becomes shorter than a quarter; that is, the maximum landward movement of the mixing zone occurs within the second quarter. *Michael et al.* [2005] identified a time lag between the seasonal freshwater-level fluctuations and the submarine groundwater discharge rate in the absence of mass transfer. Our analysis indicates that the kinetic mass transfer may alter such time lags. In addition, the cases without mass transfer show almost synchronized time lags for different contour lines, while the case with mass transfer shows significant discrepancies in time lags for different concentration contour lines: the 0.9 contour line has the shortest time lag while the 0.1 contour line the longest, resulting in the expansion of the mixing zone. Likewise, similar time lag behavior and movement discrepancies of contour lines are found in the fourth quarter for the seaward movement of the mixing zone, resulting in the contraction of the mixing zone.

[12] Figure 3c shows the mixing zone distributions for different hydraulic conductivities: 10 m d^{-1}, 30 m d^{-1} (base model), and 50 m d^{-1}. It is shown that higher hydraulic conductivity causes larger maximum and smaller minimum mixing zone thickness and more unsynchronized responses of various concentration contour lines. Mixing enhanced by mass transfer causes more significantly nonequilibrium concentrations between the mobile and immobile domain for faster flow due to enhanced timescale discrepancies between mass transfer and advection. In addition, higher hydraulic conductivities lead to larger landward and seaward movement. The impact of the amplitude of freshwater-level fluctuation is similar to that of the hydraulic conductivity because variations of the amplitude essentially change the hydraulic gradient and the flow velocity. Furthermore, given a constant total porosity, altering capacity ratio, the ratio between the immobile and mobile porosity, yields different effective mobile porosities and different flow velocities. Thus, the impact of the capacity ratio is also similar to that of hydraulic conductivity and amplitude of freshwater fluctuations.

[13] Figure 3d shows the impacts of the first-order mass transfer coefficient. The mass transfer rate coefficient controls how quickly mass is exchanged between the mobile and immobile domain. Our previous study found that when the retention timescale and the period of freshwater-level fluctuations become comparable, the mixing zone thickness is maximized [*Lu et al.*, 2009]. Three timescale ratios are considered: 0.01, 1 (base model) and 100. It is shown that narrower mixing zones are developed for the ratios 0.01 and 100, compared with the ratio 1, and their unsynchronized time lag behavior of the contour lines is similar to the case without kinetic mass transfer. Actually, mass transfer models with very small, and large mass transfer rate coefficients may be simplified to a classical advective-dispersive transport problem. For a small timescale ratio (i.e., the mass transfer is approximately equilibrium), the transport equation may be simplified by including a retardation factor. Thus, Figure 3d (left) also shows smaller displacement of the landward and seaward movement of the mixing zone. By contrast, for a large timescale ratio, i.e., the mass transfer is slow, the mass transfer between the mobile and immobile domains may be negligible and the entire system behaves approximately like a single-domain system with the effective porosity approaching the mobile porosity. As a consequence, the decreased porosity effectively speeds up the flow, resulting in a larger moving range of the mixing zone (see Figure 3d, right).

4. Conclusion

[14] Numerical experiments are conducted to investigate the dynamic behavior of mixing zone development in dual-domain media subject to periodic freshwater-level fluctuations. New findings include the following:

[15] 1. Mixing enhancement in a dual-domain coastal aquifer is mainly controlled by the unsynchronized behavior of concentration distributions in the mobile and immobile domain, the effect of which is maximized at the aquifer bottom when the retention timescale in the immobile domain is comparable to the period of freshwater-level fluctuations.

[16] 2. The effect of mixing enhancement results in nonuniform moving ranges of different concentration contour lines, nonuniform mixing enhancement, and significantly varying mixing zone thickness within one period.

[17] 3. A time lag exists between the freshwater fluctuations and the movement of the mixing zone. Such a time lag may be altered by kinetic mass transfer. By contrast, large dispersion coefficients may create thicker mixing zones but may not cause the unsynchronized behavior and alter the time lags of different concentration contour lines; that is, the mixing enhancement is rather uniform in the mixing zone.

[18] 4. The dynamics of mixing zone development is sensitive to flow velocity, which is influenced by the hydraulic conductivity, amplitude of the freshwater-level fluctuations, and the capacity ratio of mass transfer. Research is underway about implications of these findings on important physical, chemical and biological processes in coastal aquifers, such as seawater intrusion and submarine groundwater discharge.

[19] **Acknowledgments.** This research was sponsored by the National Institutes of Water Resources (NIWR) and U.S. Geological Survey (USGS) under project ID 2007GA165G. We would like to thank L. Li, H. Michael, and one anonymous reviewer for their constructive comments on the work.

References

Brovelli, A., X. Mao, and D. A. Barry (2007), Numerical modeling of tidal influence on density-dependent contaminant transport, *Water Resour. Res.*, *43*, W10426, doi:10.1029/2006WR005173.

Cartwright, N., L. Li, and P. Nielsen (2004), Response of the salt-freshwater interface in a coastal aquifer to a wave-induced groundwater pulse: Field

observations and modeling, *Adv. Water Resour.*, *27*, 297–303, doi:10.1016/j.advwatres.2003.12.005.

Cooper, H. H., F. A. Kohout, H. R. Henry, and R. E. Glover (1964), Sea water in coastal aquifers, *U.S. Geol. Water Supply Pap.*, *1613-C*.

Culkin, S. L., K. Singha, and F. D. Day-Lewis (2008), Implications of rate-limited mass transfer for aquifer storage and recovery, *Ground Water*, *46*, 591–605, doi:10.1111/j.1745-6584.2008.00435.x.

Dagan, G. (2006), Transverse mixing at freshwater saltwater interfaces: An unresolved issue, paper presented at First International Joint Salt Water Intrusion Conference—Tutorials, Univ. of Cagliari, Cagliari, Italy.

Eastwood, J. C., and P. J. Stanfield (2001), Key success factors in an ASR scheme, *Q. J. Eng. Geol. Hydrogeol.*, *34*, 399–409, doi:10.1144/qjegh.34.4.399.

Langevin, C. D., W. B. Shoemaker, W. Guo (2003), Modflow-2000, The U.S. Geological Survey modular ground-water flow model documentation of the Seawat-2000 version with the variable density flow process (VDF) and the integrated MT3DMS transport process (IMT), *U.S. Geol. Surv. Open File Rep.*, *03-426*.

Lu, C., P. K. Kitanidis, and J. Luo (2009), Effects of kinetic mass transfer and transient flow conditions on widening mixing zones in coastal aquifers, *Water Resour. Res.*, *45*, W12402, doi:10.1029/2008WR007643.

Michael, H. A., A. E. Mulligan, and C. F. Harvey (2005), Seasonal oscillations in water exchange between aquifers and the coastal ocean, *Nature*, *436*, 1145–1148, doi:10.1038/nature03935.

Robinson, C., B. Gibbes, and L. Li (2006), Driving mechanisms for groundwater flow and salt transport in a subterranean estuary, *Geophys. Res. Lett.*, *33*, L03402, doi:10.1029/2005GL025247.

Robinson, C., B. Gibbes, H. Carey, and L. Li (2007a), Salt-freshwater dynamics in a subterranean estuary over a spring-neap tidal cycle, *J. Geophys. Res.*, *112*, C09007, doi:10.1029/2006JC003888.

Robinson, C., L. Li, and H. Prommer (2007b), Tide-induced recirculation across the aquifer-ocean interface, *Water Resour. Res.*, *43*, W07428, doi:10.1029/2006WR005679.

Zhang, Q., R. E. Volker, and D. A. Lockington (2001), Influence of seaward boundary condition on contaminant transport in unconfined coastal aquifer, *J. Contam. Hydrol.*, *49*, 201–215, doi:10.1016/S0169-7722(00)00194-7.

C. Lu and J. Luo, School of Civil and Environmental Engineering, Georgia Institute of Technology, 790 Atlantic Dr. N.W., Atlanta, GA 30332-0355, USA. (jian.luo@ce.gatech.edu)